Journal of Catalysis **207,** 139–149 (2002)
doi:10.1006/jcat.2002.3515, available online at http://www.idealibrary.com on IDEAL®

Characterization and Activity of Supported Palladium Combustion Catalysts

P. O. Thevenin,*,[1] E. Pocoroba,* L. J. Pettersson,* H. Karhu,† I. J. Väyrynen,† and S. G. Järås*

*KTH—Royal Institute of Technology, Department of Chemical Engineering and Technology, Chemical Technology, Teknikringen 42, SE 10044 Stockholm, Sweden; and †University of Turku, Department of Applied Physics, FIN 20014 Turku, Finland

Received November 21, 2001; revised January 10, 2002; accepted January 16, 2002

The catalytic activity of Pd supported on γ-Al_2O_3, Ba-Al_2O_3, and La–Al_2O_3 has been examined in complete oxidation of methane when operating in excess of oxygen. Two different sizes of Pd particles have been considered. Foreign ions have a strong influence with respect to the stabilization of alumina when submitted to a temperature as high as 1000°C. In contrast, no specific effect can be detected when the samples are calcined at 500°C. Interaction with the supported palladium particles, observed during the combustion reaction, has been investigated by X-ray photoelectron spectroscopy and temperature-programmed oxidation. The difference in combustion activity is attributed to the difference in surface oxidation states of the Pd particles. The presence of foreign ions in the alumina structure results in surface PdO only. When supported on γ-Al_2O_3, small amounts of metallic Pd can be detected, resulting in a lower ignition temperature.

Key Words: **catalytic combustion; methane; palladium; alumina; metal-support interaction; TPO; XPS.**

1. INTRODUCTION

Combustion of fuel is one of the key processes in heat and power generation. A major issue related to this process is the formation of significant amounts of pollutants that occurs during the reaction between the hydrocarbons and oxygen. The main environmental concern focuses on emissions of carbon monoxide, hydrocarbons, and nitrogen oxides.

Natural gas provides an attractive source of energy since it is in abundant supply. Methane as a fuel has drawn increasing attention to various types of utilizations and has recently found application in various environmentally friendly processes. It is suitable for firing gas turbine combustion chambers (1) and has been reported as an alternative fuel for automotive applications (2).

In gas turbine applications, catalytically stabilized combustion, which was first proposed by Pfefferle (3), stabilizes the reaction of leaner fuel–air mixtures, hence lowering the adiabatic flame temperature. During the last decades, an increasing number of reviews and general articles on catalytic combustion have been published (4–8). It has been proven that emission levels below 5 ppm can be reached for the various pollutants previously mentioned (9). Besides the reduction in the CO, HC and NO_x levels in the emissions, such a technique lowers noise and vibration levels, which may cause premature damage to the gas turbine components.

In addition, the use of methane would avoid the possible formation of soot, which can be rather significant when, for instance, combusting diesel fuel. Moreover, it is a rather clean fuel with no nitrogen-bound compounds, hence avoiding the possible formation of so-called fuel–NO_x. The increasing concern about emission of greenhouse gases such as methane and carbon dioxide has been accompanied by more stringent regulations for the emissions of such compounds.

The combustion of natural gas generates more energy per mole of carbon dioxide produced when compared to other fuels (10). While the combustion of methane generates 890 kJ/mol of CO_2 produced, the corresponding value for *n*-decane and coal (graphite), for instance, are 678 and 393 kJ/mol, respectively. This property is related to the high H/C ratio, which means that methane is the most difficult hydrocarbon to oxidize. It contains only C–H bonds, which bring the molecule a rather high stability when compared to compounds containing C–C bonds (11).

Noble metal catalysts are the most active species for performing the complete oxidation of hydrocarbons. Palladium is reported to be the most active species in methane catalytic combustion, when operating under oxidizing atmosphere (12). When comparing palladium and platinum, Pd is more active for the oxidation of short-chain hydrocarbons whereas Pt exhibits higher activity toward long-chain hydrocarbons and aromatics (13).

The noble metal is usually dispersed over an inert support with a large surface area. The high temperature released during the oxidation of methane requires that the support and the catalyst maintain their integrity. The stabilization of alumina support by addition of large ions, and more specifically La, has been largely reported in the literature

[1] To whom correspondence should be addressed. Fax: +46 (0) 8 10 85 79. E-mail: philippe@ket.kth.se.

0021-9517/02 $35.00

(14–16). More recently, the influence of Nd and its interaction with PdO has been considered (17). The influence on the combustion activity of palladium seems to be affected by a possible interaction with La or Ba present in the alumina structure. The purpose of the present work is to investigate the metal–support interaction by means of different characterization techniques. Results concerning temperature-programmed oxidation (TPO) and X-ray photoelectron spectroscopy (XPS) are providing information concerning these interactions. Specific attention is given to the role of La and Ba.

2. EXPERIMENTAL

2.1. Catalyst Preparation

Palladium was deposited onto three different supports by incipient-wetness impregnation, as described elsewhere (18). Supports with the following chemical composition have been employed: Al_2O_3 (Condea, Puralox HP 14-150, 144 m^2/g), Ba–Al_2O_3 (Condea, Puralox SCFa-140 B3, 143 m^2/g), and La–Al_2O_3 (Condea, Puralox SCFa-140 L3, 142 m^2/g). The content of Ba and La, respectively, was 3 wt% for both supports. A $Pd(NO_3)_2$ solution (Alfa Aesar, 8.41 wt%) was used as the metal precursor. The volume of the impregnation solution was adjusted in order to achieve a final washcoat with a precious metal loading of 2.5 wt%.

The catalysts were dried for 12 h at 120°C prior to calcination. Subsequently, the catalyst powder was divided into two parts. One part was calcined for 4 h in air at 500°C, whereas the other portion was calcined at 1000°C.

The prepared catalysts were then coated onto a mullite tube (outer diameter, 4 mm) to test their catalytic activity in complete oxidation of CH_4. The dip coating was accomplished according to the following method: the powder to be deposited on the monolith was first dispersed in ethanol to form a slurry (dry content of 20 wt%) and ball-milled for 24 h to obtain a homogeneous suspension. The length of the catalyst layer was 30 mm, corresponding to a weight of about 20 mg. The coated catalysts are then calcined at 500°C for 4 h for the first batch and 1000°C for 4 h for the second set of catalysts to avoid any thermal deactivation during reaction.

2.2. Characterization Techniques

BET surface area. The BET surface area measurements were performed by adsorption/desorption of N_2 at the liquid nitrogen temperature. The samples were degassed in vacuum for at least 8 h at 250°C prior to adsorption measurements.

X-ray powder diffraction. The phase composition of the various samples was determined by means of X-ray powder diffraction (XRD), using a Siemens Diffraktometer 5000. The operating parameters were monochromatic Cu-K_α radiation, Ni filter, 30 mA, 40 kV, 2θ scanning from 20 to 80°, and a scan step size of 0.02. Phase identification was done using the reference database (JCPDS-files) supplied with the equipment.

Transmission and scanning electron microscopy. The morphology, size, and dispersion of the palladium particles on the alumina washcoat were studied using a transmission electron microscope (TEM—JEOL 2000 FX) operated at 200 kV and a scanning electron microscope (SEM—Zeiss DSM 940) operated at 20 kV. The TEM microscope was equipped with an EDS (energy dispersive spectroscopy) detector (LINK AN 10000). The SEM microscope was equipped with an EDS detector (LINK QX 2000).

Temperature-programmed oxidation. The redox properties of the samples were measured by means of temperature-programmed oxidation (TPO) experiments on a Thermoquest TPD/R/O 1100 equipped with a thermal conductivity detector (TCD). Approximately 100 mg of calcined powder was used for each measurement. Prior to TPO experiments, the samples were reduced in a 5% H_2/Ar atmosphere. Subsequently, TPO experiments have been performed using a gas mixture of 2.12% O_2/He with a flow rate of 30 $cm^3 \cdot min^{-1}$, increasing the temperature from 25 to either 500 or 1000°C depending on the calcination temperature of the sample, at the rate of $10°C \cdot min^{-1}$.

X-ray photoelectron spectroscopy. The calibration of the binding energy (BE) was based on the carbon impurity peak at 284.6 eV. Samples were charged approximately 5 eV in the X-ray bombardment, but we did not observe changes in charging during the typically 7-h measurement time. The acquisition time of 7 h was employed in order to improve the signal-to-noise ratio, as due to the relative high surface area and the small particle size the photoelectron intensity was very low. Therefore, at least 20 scans were performed at the rate of 1 eV/s, in the desired energy range. The depth of the analysis was about 1–20 Å. In the computer fitting procedure of spectra with multiple states due to spin–orbit interaction, intensity ratios and energy separations of states were kept constant at the theoretical values. Shirley background due to inelastic photoelectron scattering was removed prior to Voigt function peak fitting. A pass energy of 35 eV was used, with typically 1×10^{-8} Torr pressure during the analysis. A Perkin–Elmer PHI 5400 ESCA was used, with a nonmonochromatized Mg K_α source, using 100 W of power to prevent sample reduction during the X-ray bombardment. Impurities other than carbon were not observed. Sensitivity factors used in quantitative analysis for Al 2p, Ba $3d_{5/2}$, La 3d, O 1s, and Pd 3d were 0.234, 7.469, 9.122, 0.711, and 5.356, respectively (19). The accuracy of the BE values is ca. ±0.15 eV.

2.3. Activity Tests

Activity tests were performed on catalysts coated on a mullite tube, located in an annular reactor, as described elsewhere (20). The use of such annular reactors was first proposed by McCarty (21) and has since been widely reported in the literature (22, 23). It is made of quartz and placed in an 800-mm-long furnace. A K-type thermocouple is inserted in the mullite tube in order to measure the catalyst temperature during combustion experiments.

During the transient experiments, a furnace heating-rate of $3°C \cdot min^{-1}$ was used. The total gas flow-rate was 0.94 $dm^3 \cdot min^{-1}$, resulting in a linear gas velocity of $1.0\,m \cdot s^{-1}$, with a fuel concentration of 1 vol% CH_4 in air.

The composition of the product gas was monitored by online gas chromatography (GC Varian 3800) equipped with a TCD. The conversion calculations are based on the concentration of CH_4 and corroborated by the yields of CO_2 and CO.

3. RESULTS

3.1. Surface and Bulk Properties of the Prepared Catalysts

The results concerning BET measurements, TEM and SEM observations, and selected XPS measurements are reported in Tables 1 and 2.

BET surface area. After calcination at 500°C, all samples present similar surface properties with a surface area of about 144 $m^2 \cdot g^{-1}$, as seen in Table 1. No major difference can be observed between the pure alumina and the smaples containing Ba or La.

When submitted to further calcination, up to 1000°C, the measurements of the BET surface area of the stabilized alumina reflect the significant influence of La or Ba. This effect becomes noteworthy when the calcination temperature reaches 1000°C. The surface area of the nondoped sample undergoes a sharp decrease after calcination at 1000°C due to sintering, showing a specific surface area of only 75 $m^2 \cdot g^{-1}$.

In contrast, the materials containing La or Ba maintain a notably higher surface area, when compared to neat alumina, and the modified supports exhibit a surface area in the range 95–105 m^2/g. The presence of La or Ba is effective in reducing the strong sintering of alumina. La is more effective in thermally stabilizing alumina, probably due to its larger ionic diameter (14), compared to Ba.

X-ray powder diffraction. The objective of the XRD measurements was to (a) examine the nature of the Pd particles and (b) investigate the possible modifications of the alumina-based washcoat. Special attention is given to the possible formation of La and Ba mixed oxides as well as to changes in the alumina phases. Concerning the identification of crystalline structures of Pd, the focus of attention was the oxide form, PdO, as it is the most active species

TABLE 2

Atomic Surface Composition of the Samples after Calcinations at 500 and 1000°C, Determined by XPS analysis

Temperature	Pd/Al_2O_3 (Pd : Al)	$Pd/La–Al_2O_3$ (Pd : La : Al)	$Pd/Ba–Al_2O_3$ (Pd : Ba : Al)
	0.013 : 1[a]	0.013 : 0.012 : 1[a]	0.013 : 0.012 : 1[a]
500°C	0.12 : 1	0.084 : 0.27 : 1	0.054 : 0.31 : 1
1000°C	0.0017 : 1	0.00089 : 0.026 : 1	0.0012 : 0.022 : 1

[a] Calculated bulk atomic ratio.

TABLE 1

Surface Properties of the Different Prepared Catalysts

Sample	Calcination temperature (°C)	Surface area[a] (m^2/g)	Pd particle size[b] (nm)	Binding energy[c] (eV)			
				Pd $3d_{5/2}$	La $3d_{5/2}$	Ba $3d_{5/2}$	Al 2p
Pd/Al_2O_3	500	144	5–10	334.9 (36%) 336.4 (64%)	—	—	74.5
$Pd/Ba–Al_2O_3$	500	143	5–10	334.9 (24%) 336.2 (76%)	—	780.5	74.2
$Pd/La–Al_2O_3$	500	142	5–10	334.9 (48%) 336.5 (52%)	835.5 839.1	—	74.3
Pd/Al_2O_3	1000	75	80–100	334.9 (13%) 336.5 (87%)	—	—	73.8
$Pd/Ba–Al_2O_3$	1000	94	80–100	336.8	—	780.7	74.1
$Pd/La–Al_2O_3$	1000	107	80–100	336.7	835.9 839.2	—	74.2

[a] Measured by BET.
[b] Determined by TEM.
[c] All BEs referenced to C 1s = 284.6 eV.

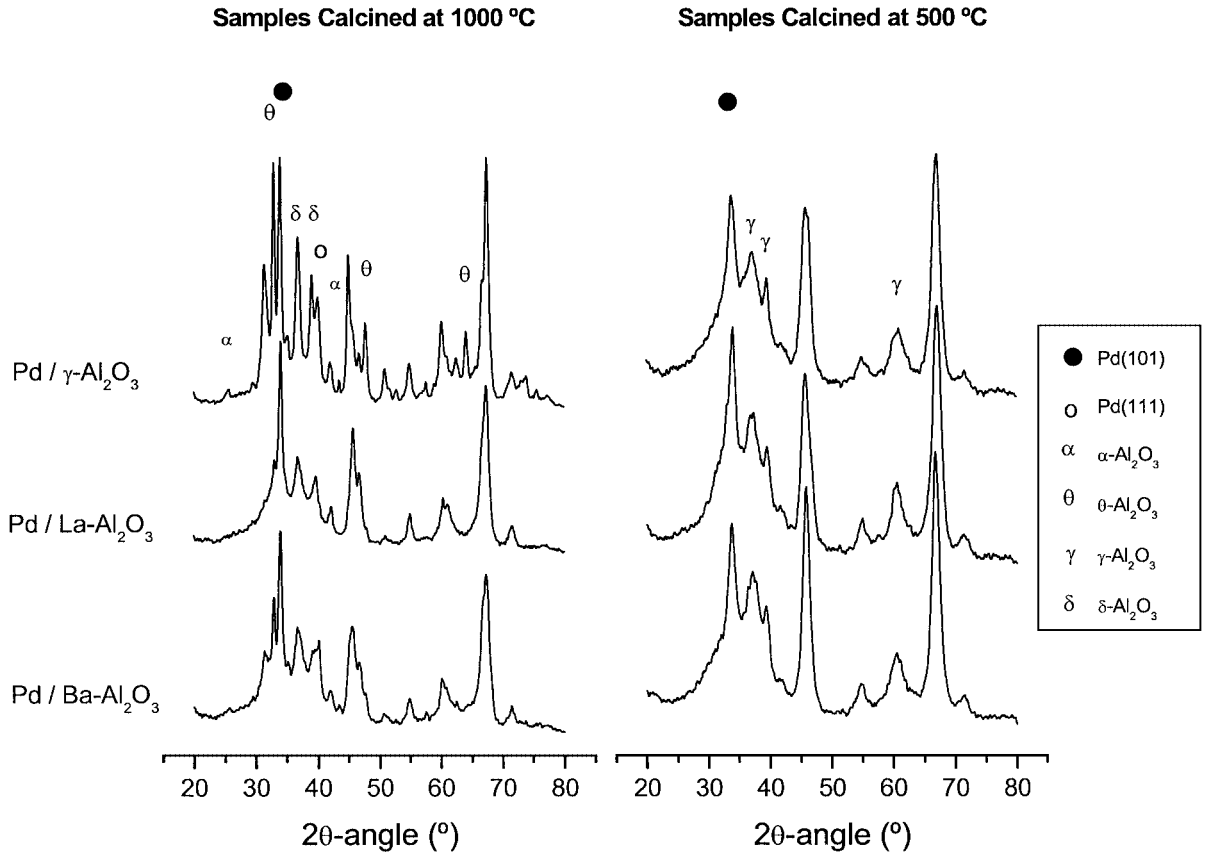

FIG. 1. Comparison of the X-ray diffractogram of pure alumina with stabilized alumina after calcination at 500 and 1000°C.

for the complete oxidation of methane, when operating in excess of oxygen.

The tetragonal form of Pd was identified by its XRD reflection at $2\theta = 33.889°$ for the (101) plane and $2\theta = 54.759°$ for the (112) plane. The cubic Pd^0 was identified by its XRD reflection at $2\theta = 40.115°$, (111) plane, and 82.096°, (222) plane. Owing to the overlapping of alumina and Pd reflections, the other main peaks of PdO (41.948 and 60.207°) and of Pd^0 (46.682°) could not be used for structure determination.

We observed that the PdO peak for the samples calcined at 500°C is rather small and broad, reflecting the presence of small crystalline particles of PdO (cf. Fig. 1). On calcination at 1000°C, the shape of the peak becomes sharper and more intense, corresponding to an increase in size of the crystalline particle. Despite the calcination at 1000°C in air, we can still detect the presence of small amounts of cubic Pd(111). Nevertheless, palladium particles exhibit a rather high PdO/Pd ratio with respect to the crystalline phases, as seen by comparing the intensity of the reflection at $2\theta = 33.889°$ and $2\theta = 40.115°$.

The La- and Ba-modified aluminas exhibit similar XRD patterns after calcinations at both 500 and 1000°C. It seems that the increase in PdO particle size is comparable as well, despite the different composition of the support materials.

The first observable effect of the crystal structure is calcination temperature (cf. Fig. 1). An increase from 500 to 1000°C gives rise to the formation of more crystalline PdO for all samples, with a more intense peak at $2\theta = 34°$. After calcination at 500°C PdO is already present in a crystalline state, at least partially. A similar observation can be made concerning the crystal structure of alumina. When raising the calcination temperature, the peaks of alumina and Pd develop into sharper and more intense ones, reflecting an important crystal growth, which in the case of alumina may be accompanied by a decrease in the specific surface area of the support material.

In contrast, an important difference is observed when comparing the XRD pattern of the pure alumina and Ba- or La-stabilized alumina. The pure alumina undergoes severe modification of its crystalline structure under calcination at 1000°C, whereas in the presence of additives the transformation of the Al_2O_3 structure is lower. As reported in the literature (24), the alumina undergoes the following phase transformation when increasing the calcination temperature (see Fig. 2).

Concerning the phase transformation, solid-state diffusion occurs within the defects of the crystal lattice. Atoms, ions, or vacancies can move via these defects to a lower energy state, and such movements may be associated with

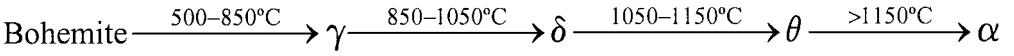

FIG. 2. Modification of the crystal phase of alumina under increasing calcination temperatures.

phase transformation. The presence of voluminous elements within the crystal lattice of alumina strongly lowers the mobility of the atoms (25).

These transformations are clearly observed on the pure alumina samples as well. The most evident aspect of these changes is the emergence of a θ-Al_2O_3 peak, simultaneously with the increase in intensity of the δ-Al_2O_3 diffraction peak (when compared to the Pd peaks that have a similar intensity regardless of the nature of the support). When considering the samples containing Ba or La ions, these changes are not that marked and the alumina tends to remain in the γ-Al_2O_3 crystal phase.

The addition of Ba or La stabilizes the alumina material against changes in crystal phase, as reported in earlier literature (24). This commercial support, with a La or Ba content of about 3 wt%, exhibits stable behavior, even after calcination at 1000°C for 4 h. In comparison, neat alumina shows an intense modification of the crystal structure. The samples calcined at 500°C are mostly amorphous whereas further calcination up to 1000°C causes a severe crystal growth that is accompanied by a decrease in the BET surface area.

Transmission and scanning electron microscopy. The results from the microscopy analyses show that the Pd particles are present in two distinct sizes, resulting from the two different calcination temperatures. The samples calcined at 500°C for 4 h contain Pd particles that have a diameter in the range of 2–5 nm whereas the catalysts calcined at 1000°C exhibit much larger particles, in the range 80–100 nm. In both cases, an even Pd dispersion over the support material was noticed regardless of the nature of the support. No substantial concentration of Pd particles could be detected.

Due to the detection limit of the SEM microscope, the analysis of the samples concerned only the catalyst calcined at 1000°C. The catalysts show well-dispersed palladium particles on the washcoat material (cf. Figs. 3A–3C), independent of the nature of the support material. We did not observe any large agglomerate of Pd particles or any strong discrepancy in particle size. This result corroborates the analysis made with the TEM microscope. In this case, the higher resolution enabled us to observe even particles as small as about 5 nm. The detection limit of the TEM (ca. 1 nm) did not allow the observation of smaller particles.

In addition to the behavior of the metal particles, sintering of the support material can be observed. We can observe that the size of the alumina particles increases when raising the calcination temperature from 500 to 1000°C. In contrast,

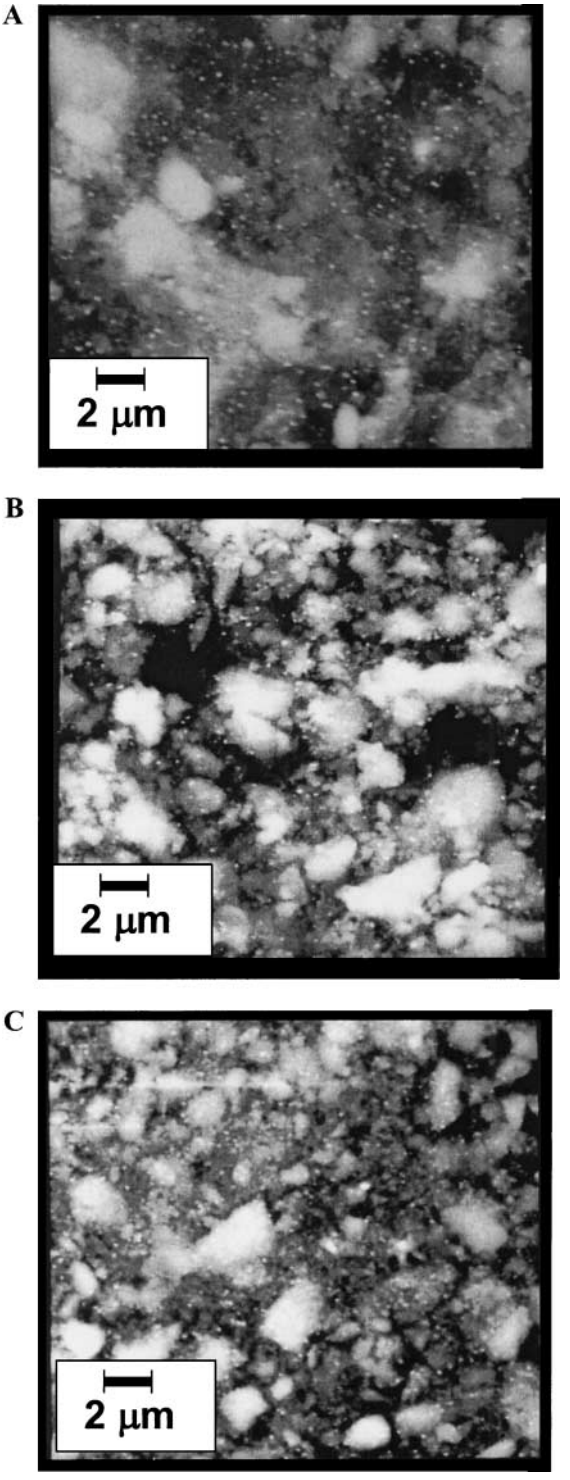

FIG. 3. SEM photograph of the samples calcined at 1000°C, supported on the different materials. (A) Al_2O_3, (B) La-stabilized Al_2O_3, and (C) Ba-stabilized Al_2O_3.

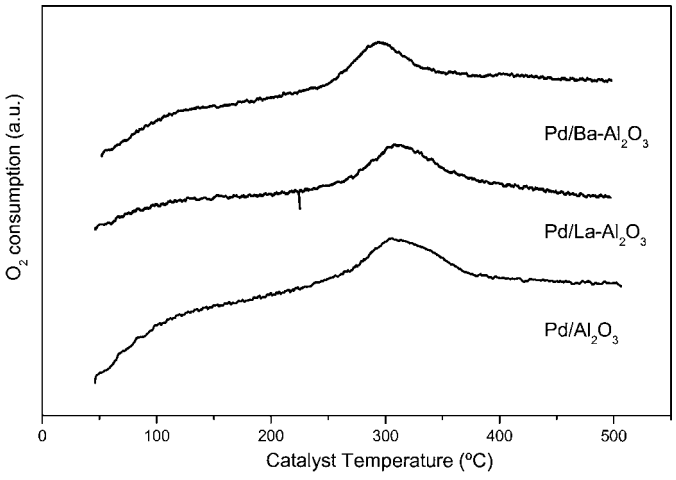

FIG. 4. TPO experiments on samples calcined at 500°C for 4 h.

the samples containing rare earth elements are not subject to such modification.

Temperature-programmed oxidation. The purpose of the TPO experiments was to investigate the behavior of supported Pd catalysts under oxidative conditions. Specific attention is given to the PdO–Pd decomposition that takes place at about 750–800°C. Temperature-programmed oxidation experiments were completed over the samples calcined at 500°C (Fig. 4) and 1000°C (Fig. 5). During the TPO performed on the samples calcined at 500°C, similar O_2 profiles are observed, in spite of the nature of the support. We observed a single peak of O_2 consumption at about 300°C. The peak is relatively wide, reflecting an O_2 consumption that takes place over an extended temperature window. This O_2 consumption starts at about 250°C and the oxidation is complete at 350°C. A similar observation can be made for the various catalysts in spite of the different nature of the support materials.

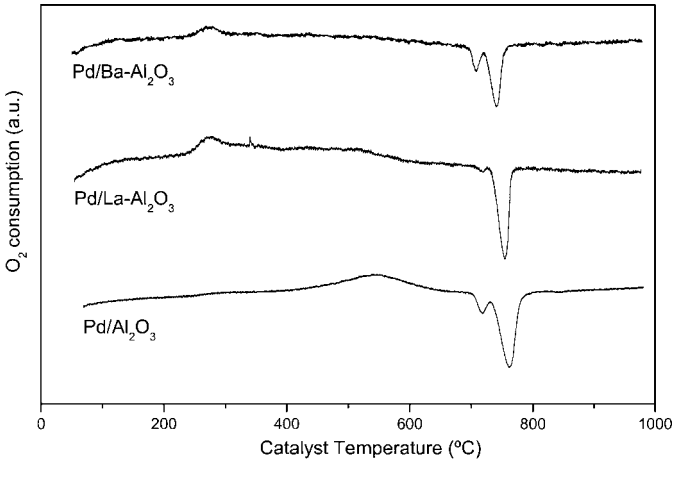

FIG. 5. TPO experiments on samples calcined at 1000°C for 4 h.

In contrast, the samples calcined at 1000°C exhibit singular patterns, depending on the chemical composition of the washcoat. The samples supported on stabilized alumina present a first peak with a maximum at about 300°C, representing the oxidation of Pd species. The oxidation starts as soon as the temperature of the catalyst is increased. When supported on pure alumina, the oxidation of Pd reaches a maximum at 500°C only. Complete oxidation is however reached at a similar temperature, i.e., 600°C. The palladium-free supports do not present any significant activity during TPO experiments (26). The variations between the different catalysts with respect to their TPO profiles can therefore be attributed to the modifications in metal–support interaction by the stabilizers, La and Ba.

Negative peaks represent an O_2 "desorption" when increasing the temperature up to 800°C. This occurs in two successive and distinctive steps: a first one at about 720°C followed by a second, more intense one at ca. 750°C. This decomposition of PdO into metallic Pd is the cause of this behavior. These two steps observed are directly connected to the two types of PdO, as previously reported (26). PdO seems to be present in a bulk form (27) and a surface complex oxide form (21), the later being decomposed at lower temperatures than the former.

It is important to notice that when supported on La–Al_2O_3, the decomposition of PdO takes place in one main step only, with a major peak at 755°C. A first peak is still detectable at 715°C, but its intensity is negligible when comparing the TPO profiles measured over the other catalysts.

X-ray photoelectron spectroscopy. It seems that the presence of La and Ba additives causes a raise in the binding energy of palladium in the samples calcined at 1000°C, as seen in Table 1. After calcination at 500°C this phenomenon was not observed, which indicates that a temperature of 500°C is not high enough to bring about a strong interaction of Ba or La ions with Pd. In addition, binding energies give evidence that samples calcined at 1000°C were slightly more oxidized than the samples calcined at 500°C. The samples containing additives do not present any metallic Pd contribution in the XPS spectra, whereas the neat Al_2O_3 support reflect the presence of about 13% Pd^0. Furthermore, the samples calcined at 500°C and Pd/alumina calcined at 1000°C show the presence of small amounts of Pd^0. Most likely, the reduction was due to X-ray bombardment in ultrahigh vacuum conditions, which only the two most stable catalysts were able to fully endure.

We observed 780.5–780.7 eV binding energies for barium $3d_{5/2}$, which is in good agreement with the results published by Talo *et al.* (28). This BE actually corresponds to the literature value of Ba^0, the metallic bulk barium value. However, metallic Ba in the literature has a strong satellite line at ca. 787 eV, which is significantly weaker for this catalyst. Most likely this BE originates from BaO in the dispersed state. Comparison of the two Pd/Ba–Al_2O_3 catalysts at the

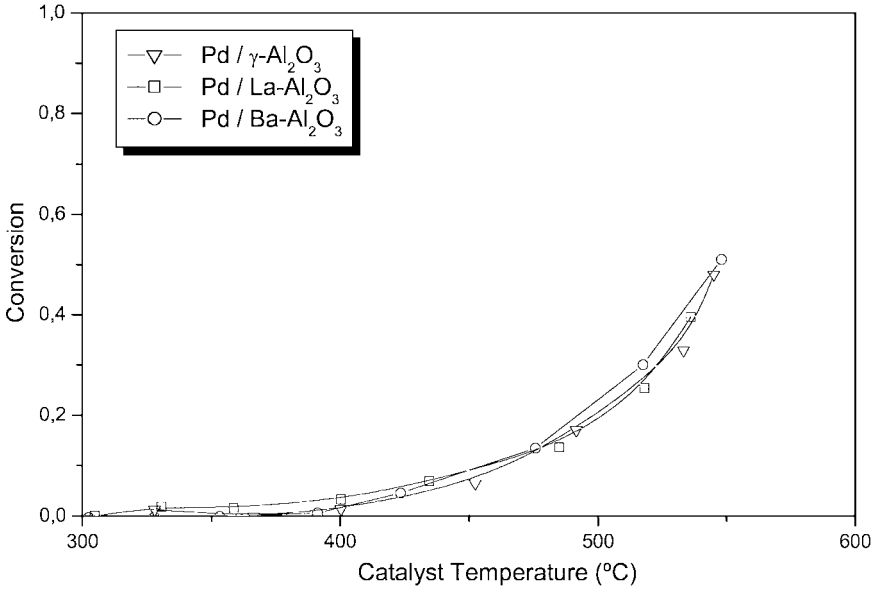

FIG. 6. Combustion activity of the catalyst after calcination at 500°C.

two different calcination temperatures, in Table 2, shows a 93% drop in surface Ba atomic concentration when the calcination temperature was raised to 1000°C.

The BEs of lanthanum in both catalysts with different calcination temperatures were in agreement with previous studies of dispersed lanthanum, i.e., 835.0–836.1 eV (28, 29). Our initial lanthanum-loading, La/Al ratio was 0.27, which can be compared to the range 0.25–0.50 in the work by Haack *et al.* (29). In this loading range, according to Bettman *et al.* in their XRD studies (30), lanthanum remains well dispersed in the form of surface lanthanum aluminate, $LaAlO_3$. At higher La/Al ratios, ranging from 0.75 to 2.0, Haack *et al.* observed the Al 2p peak at 73.0 eV, which corresponds to Al in $LaAlO_3$. In our XPS experiments we observed that the Al 2p BEs were slightly lower for the samples calcined at the higher temperature, which is due to the increased formation of $LaAlO_3$, probably in crystalline form. While the bulk concentrations of La are similar in the catalysts calcined at 500 and 1000°C, the atomic-surface La/Al ratio after calcination at the higher temperature was only ca. 10% of the ratio in the catalyst calcined at the lower temperature. This is due to the increased agglomeration of Al at the higher temperature, which also may lead to the formation of $LaAlO_3$ crystals. The BEs for the La $3d_{5/2}$ line are higher than 835 eV, which is attributed to one form of surface lanthanum (28, 29, 31). When the size of the particles increases, dispersion should weaken but we observed only 0.4 eV change in BE toward bulk La_2O_3, which is still well dispersed in the La BE range. The O 1s line was found at 531.3 eV in the Pd/Al_2O_3 and $Pd/La–Al_2O_3$ samples calcined at 1000°C without any additional shoulders, which is characteristic of O in Al_2O_3, but does not offer any additional information regarding La and Al. This is in agreement with the results reported by Haack *et al.* in the case of La-stabilized alumina, with a low La/Al ratio.

3.2. Activity Tests

Results of the activity tests over the various catalysts are represented in Fig. 6 for the samples calcined at 500°C and Fig. 7 for the ones calcined at 1000°C.

For the samples calcined at 500°C, no major differences are observed with respect to the catalytic activity of Pd-supported catalysts in complete oxidation of methane. Pd/Al_2O_3, $Pd/La–Al_2O_3$, and $Pd/Ba–Al_2O_3$ present similar combustion activity regardless of the nature of the support material. We observe an ignition of the fuel–air mixture that starts at about 470°C (T_{10}, temperature for 10% conversion) and 50% conversion is reached at about 550°C. In addition, the apparent reaction rate for the complete oxidation of methane is similar over the three concerned catalysts.

In contrast, the catalysts calcined at the higher temperature (1000°C) and presenting larger Pd particles have a combustion activity that seems to be directly influenced by the chemical composition of the support. In fact, the use of γ-alumina as a support for Pd particles brings a higher activity when compared to the use of stabilized aluminas. There is a difference of at least 100°C with respect to the T_{10} and T_{50} values. The catalysts supported on stabilized alumina have a similar ignition behavior until the catalyst temperature reaches 620°C. In the temperature window 620–800°C, a higher apparent reaction rate over the $Pd/La–Al_2O_3$ catalyst is observed when compared to the $Pd/Ba–Al_2O_3$ system. When the temperature is further increased, they retrieve an identical apparent reaction rate.

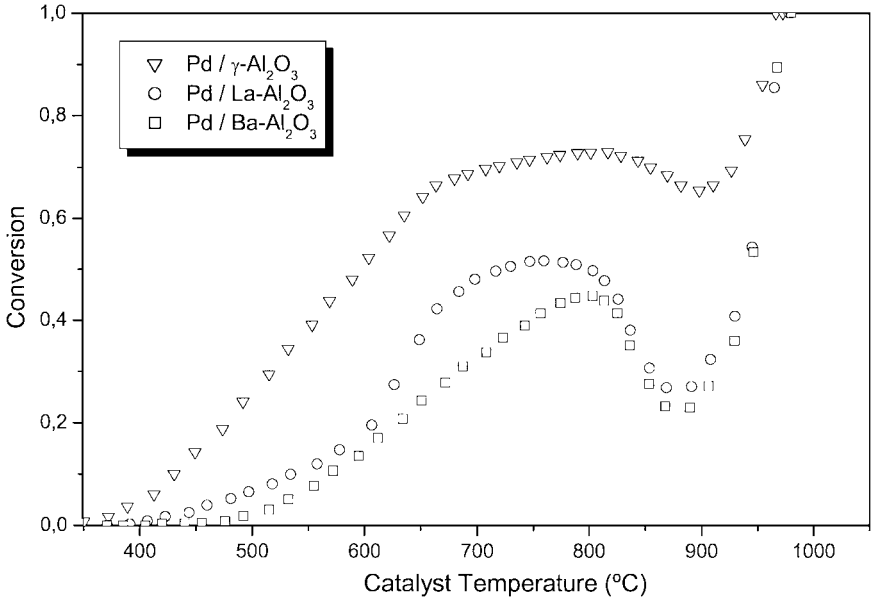

FIG. 7. Combustion activity of the catalyst after calcination at 1000°C.

The decrease of combustion activity due to the PdO decomposition takes place at about 800°C for the three catalysts but is more pronounced over the catalysts supported on Ba- and La-stabilized alumina.

4. DISCUSSION

4.1. Structure of the Washcoat—Effect of La and Ba on the Stability of Al_2O_3

Materials that have different chemical composition were used to support palladium particles. The calcination of the catalyst powders was performed at two distinctive temperatures. In that way, we achieved catalysts with palladium particles of different size, in order to investigate the metal–support interaction with respect to the metal particle size and the nature of the support material.

The rate of sintering is an activated process with a diffusion coefficient that is exponentially dependent on temperature. The surface diffusion becomes significant near the Hüttig temperature (~0.3 T_m K). When the temperature further increases near the Tammann temperature (0.5 T_m K), volume diffusion starts, and migration of interstitials (Frenkel effect) or vacancies (Shottky effect) may be involved. For instance, the addition of rare earth elements such as La has been reported to be suitable for inhibiting these diffusion processes (24). Sintering may occur via various diffusion processes: surface, volume, and/or grain boundary diffusion (32, 33). The resistance to sintering of the catalyst supports is clearly improved by addition of even small amounts of large ions such as barium or lanthanum. These large ions (such as +), located in the alumina crystal lattice, hinder or at least retard these diffusion processes. This results in a larger BET surface area when compared to pure alumina. In addition, the alumina particles observed by TEM are smaller. The influence of this addition of La or Ba is observable as well when examining the crystal structure of the support material. In parallel to the decrease in surface area, the alumina support undergoes modification of its crystal phase. The presence of new phases (θ-Al_2O_3, δ-Al_2O_3, and traces of α-Al_2O_3) are noticed when pure alumina is calcined at 1000°C, whereas γ-Al_2O_3 is the dominating phase after thermal treatment at 500°C. In contrast, the samples containing the foreign ion exhibit the initial crystal phase, γ-Al_2O_3, after calcinations at both 500 and 1000°C.

However, besides this clear positive effect on the thermal stability of alumina material, the presence of foreign ion elements has a noteworthy effect on the properties of Pd species. This is observed both by XPS analysis and through evaluation of the catalytic activity in methane combustion.

When investigating the XPS line for La, the binding energy is the same as the one for La in surface $LaAlO_3$. The XPS measurements indicate the presence of La in the form of $LaAlO_3$. This phase is however not detected during XRD analysis. This comparison of the results obtained by XRD and XPS, with respect to the existence of La, leads to the conclusion that the size of the particles is probably below the XRD detection limit (ca. 2 nm), at least for the La present in the outer layer (1–20 Å). Similar observations are made concerning the Ba particles. In addition, we measure a decrease in surface atomic concentration in La and Ba when raising the calcination temperature from 500 to 1000°C.

The observed results are in agreement with previous findings in the literature reporting on the stabilizing effect of

rare earth additions (14, 15). The BET surface area measurements are corroborated by the X-ray diffraction patterns that exhibit the strong influence of foreign ions on the thermal stability of the alumina supports.

4.2. Structure of Pd—Effect of Addition of La and Ba

Considering the investigation of the palladium particles, their size is apparently not affected by the presence of La and Ba in the alumina support. Both microscopy examinations and XRD study show that the size of the palladium particles is identical and they are well dispersed at the surface of the support. The TEM observation showed that the Pd particles sinter considerably when the calcination temperature is raised from 500 to 1000°C. Similar conclusions can be drawn from the XRD pattern where the peak of the PdO reflection increases in intensity and getts sharper. This increase in palladium particle size is not affected by the nature of the support material on which the metal particles have been deposited. Furthermore, the intensity and shape of the PdO peaks are similar in the different samples considered.

In the three samples calcined at 500°C reported in Table 2, the binding energy value of Pd $3d_{5/2}$ corresponds to PdO. It matches results by Shyu *et al.* (34) and also Otto *et al.* (35). Shelef *et al.* (36) observed similar PdO binding energies on Pd/La-sapphire samples after oxidation at 600°C. No PdO_2 at 338.3 eV, as measured by Otto *et al.* (35), is present in our samples. In addition, the surface atomic concentration measured by XPS reflects the encapsulation of Pd when increasing the calcination temperature. We notice a strong decline in the amount of Pd, Ba, and La accessible at the surface, while the concentration of Al rises considerably. This probably explains the lower activity of the samples calcined at 1000°C when compared to the samples treated at a lower temperature. In addition, the influence of Ba and La with respect to the Pd particles is not observed when considering the bulk properties. The XRD analysis displays similar patterns regardless of the nature of the support on which the palladium is dispersed. This is in agreement with the TEM and SEM observations that imply that the size of the Pd particles is identical for all the catalysts calcined at the same temperature. The size of the Pd particles is about 80–100 nm for the samples calcined at 1000°C. The initial size, after calcination at 500°C, is in the 2- to 5-nm range. The presence of small amounts of metallic Pd is observed by XRD.

As opposed to the above results, the surface characterizations (XPS, TPO, and combustion experiments) reflect a much stronger influence of the additives. By XPS, for instance, we notice a shift in the PdO peak toward the higher binding energy when the samples contain Ba or La. The stronger effect is observed for the catalyst supported on La-stabilized alumina. The oxidation state is then affected by the presence of La or Ba and only PdO is present at the surface of the catalyst calcined at 1000°C, when supported on the modified alumina. The reduction of Pd can be due to the photoelectron beam as well. The shift is observed on the samples calcined at 1000°C only. The XPS line for Pd in the samples calcined at 500°C is at the same binding energy, in spite of the chemical composition of the support. Nevertheless, the TPO experiments (Fig. 5) suggest an influence of Ba and La as well. Just as for the XPS analysis, the effect is observable only when the samples are calcined at 1000°C, as the samples calcined at 500°C present almost identical TPO profiles.

The catalytic activity of the various catalysts in complete oxidation of methane is illustrated in Figs. 6 and 7. In Fig. 6, the activity of small particles (calcined at 500°C) is displayed whereas Fig. 7 exhibits the activity of larger particles (calcined at 1000°C), both in complete oxidation of methane.

The activity of the small particles is apparently not affected by the various natures of the support material. The presence of rare earth elements in the alumina matrix does not affect the catalytic activity of the supported PdO particles. All the different catalysts present a similar ignition path, with a difference in T_{50} and T_{10} of fewer than 10°C. On the other hand, it seems that the large particles present singular behavior for each support. The neat alumina provides a lower ignition temperature whereas the use of La- and Ba-stabilized Al_2O_3 materials requires a higher catalyst temperature to reach similar conversion. The catalyst supported on neat alumina displayed a T_{50} of about 450°C. On the other hand, the modified alumina supports require an inlet temperature of about 530 and 550°C for Ba–Al_2O_3 and La–Al_2O_3, respectively, to reach a methane conversion of 50%.

During the combustion of methane over palladium-based catalysts, a decrease in activity is observed at about 750°C. This phenomenon has been largely reported in the literature and is due to the decomposition of active palladium oxide, PdO, into less active metallic palladium (21, 37, 38). In addition to the increase in ignition temperature observed over the modified support materials, the decrease in methane combustion activity, observed at about 800°C, exhibits different intensity with respect to the nature of the washcoat. The loss of combustion activity is much more intense when the oxidation takes place over Pd/Ba-stabilized Al_2O_3 or Pd/La-stabilized Al_2O_3, when compared to the Pd/Al_2O_3. The decomposition rate of PdO into less active Pd is increased by the presence of La or Ba in the support. This is probably due to differences in acidity of the support, as the basicity of the support may follow the decreasing order Ba–Al_2O_3 > La–Al_2O_3 ≫ Al_2O_3.

When the particles are larger, the catalysts have different ignition behavior depending on the nature of the support. The alumina-supported catalysts, despite a lower surface area, are much more active than the samples

impregnated on thermally stable materials. This is probably due to a difference in palladium oxidation state when compared to the samples containing Ba or La. In addition, the presence of metallic Pd for the samples dispersed on alumina may enhance the oxidation of methane, as Pd is responsible for the dissociation of methane (13). The absence of such Pd^0 when La or Ba are present is responsible for the lower combustion activity. Moreover, it is possible to distinguish the catalysts with respect to the nature of the ion that has been employed to stabilize the alumina support. The Pd/Ba-stabilized Al_2O_3 catalyst, calcined at 1000°C, exhibits a lower combustion activity than Pd/La-stabilized Al_2O_3, even if the surface areas of the supports are in the same order of magnitude. In that case, the interaction between the palladium particles and La or Ba atoms seems responsible for this specific behavior. The surface property measurements (XPS, TPO) exhibit results that confirm this hypothesis.

5. CONCLUSIONS

Pd-based catalysts have been prepared by impregnation of three different support materials. Two of them contain rare earth ions, Ba and La. The presence of La or Ba improves the thermal stability of alumina support when exposed to temperature as high as 1000°C. The supports containing 3 wt% of La or Ba maintain a BET surface area of about 95 m^2/g after calcination at 1000°C, whereas the pure alumina displays a more intense sintering with a surface area of only 75 m^2/g.

The presence of Ba or La retards the strong sintering of the alumina support, as confirmed by BET and XRD measurements. In contrast, the presence of these foreign ions exhibits a negative effect with respect to the combustion activity.

The increase in calcination temperature from 500 to 1000°C mainly affects the surface composition and properties of the catalysts. Calcination at 500°C leads to catalysts with almost identical properties. In contrast, when increasing the calcination temperature to 1000°C, significant changes are observed in both surface composition and behavior. One of the most important is the sintering of both the support and the noble metal particles.

In addition, we notice a strong modification of the surface chemical composition, with an important decrease in Pd concentration. The Al ions migrate to the outer surface of the catalyst, and a decrease in Pd, La, and Ba accessibility is measured. This entails an increase in the interaction of the Pd with the support material, and especially the La and Ba present in the alumina structure. Results from X-ray photoelectron spectroscopy proved as well that La and Ba, after calcination at 1000°C, inhibit the formation of a mixed phase in which Pd in both the metallic and oxide phase is present. This latter combination is the most active for the complete oxidation of methane when operating in excess oxygen.

The increase in the apparent reaction rate observed between 600 and 700°C for the catalyst supported on La–alumina is confirmed by the TPO experiments. The decomposition of PdO into metallic and less active Pd starts at higher temperature. Only one peak in the higher temperature region is observed.

The large Pd particles exhibit stronger interaction with Ba and La, respectively, as Ba and La are in the form of small oxide particles well dispersed in the alumina matrix. There is much more interaction between the Pd particles and the foreign ions present in Al_2O_3 than in the case of small and well-dispersed Pd particles. When increasing the calcination temperature, different effects can be observed with respect to the catalytic properties. The foreign ions retard the sintering of the alumina support but result in a lower combustion activity due to the absence of the mixed Pd–PdO phase.

ACKNOWLEDGMENTS

STEM—the Swedish National Energy Administration—is acknowledged for financially supporting this work. Thanks are due to Condea GmbH for providing the alumina supports. The authors would also like to thank Dr. M. Ferrandon and Prof. P. G. Menon for valuable discussions and comments.

REFERENCES

1. Pfefferle, L. D., and Pfefferle, W. C., *Catal. Rev.* **29**, 219 (1987).
2. Bell, S. R., SAE Paper 931829.
3. Pfefferle, W. C., Belgian Patent 814,752 (1974).
4. Zwinkels, M. F. M., Järås, S. G., Menon, P. G., and Griffin, T. A., *Catal. Rev.* **35**, 319 (1993).
5. Johansson, E. M., Papadias, D., Thevenin, P. O., Ersson, A. G., Gabrielsson, R., Menon, P. G., Björnbom, P. H., and Järås, S. G., *in* "Catalysis—Specialists Periodical Reports" (J. J. Spivey, Ed.), Vol. 14, p. 183. Royal Society of Chemistry, Cambridge, 1999.
6. Eguchi, K., and Arai, H., *Catal. Today* **29**, 379 (1996).
7. Forzatti, P., and Groppi, G., *Catal. Today* **54**, 165 (1999).
8. Hayes, R. E., and Kolaczkowski, S. T., "Introduction to Catalytic Combustion." Gordon & Breach, Amsterdam, 1997.
9. Dalla Betta, R. A., *Catal. Today* **35**, 129 (1997).
10. Chin, Y. H., and Resasco, D., *in* "Catalysis—Specialists Periodical Reports" (J. J. Spivey, Ed.), Vol. 14, p. 1. Royal Society of Chemistry, Cambridge, 1999.
11. Epling, W. S., and Hoflund, G. B., *J. Catal.* **185**, 5 (1999).
12. Briot, P., and Primet, M., *Appl. Catal.* **68**, 301 (1991).
13. Burch, R., and Hayes, M. J., *J. Mol. Catal. A* **100**, 13 (1995).
14. Schaper, H., Doesburg, E. B. M., and Reijen, L. L. V., *Appl. Catal.* **7**, 211 (1983).
15. Beguin, B., Garbowski, E., and Primet, M., *Appl. Catal.* **75**, 119 (1991).
16. Chen, X., Liu, Y., Niu, G., Zhuxian, Y., Maiying, B., and Adi, H., *Appl. Catal. A* **205**, 159 (2001).
17. Suhonen, S., Valden, M., Pessa, M., Savimäki, A., Härkönen, M., Hietikko, M., Pursiainen, J., and Laitinen, R., *Appl. Catal. A* **207**, 113 (2001).
18. Geus, J. W., *in* "Preparation of Catalyst III" (G. Poncelet, P. Grange, and P. A. Jacobs, Eds.), p. 1. Elsevier Science, Amsterdam, 1983.

19. Moulder J. F., Stickle, W. F., Sobol, P. E., and Bomben, K. D., "Handbook of X-Ray Photoelectron Spectroscopy." Perkin–Elmer, Physical Electronics Division, Eden Prairie, MN, 1992.
20. Papadias, D., Würtenberger, U., Edsberg, L., and Björnbom, P., *Chem. Eng. Sci.*, in press.
21. McCarty, J. G., *Catal. Today* **26**, 283 (1995).
22. Groppi, G., Ibashi, W., Tronconi, E., and Forzatti, P., *Chem. Eng. J.* **82**, 57 (2001).
23. Johansson, E. M., and Järås, S. G., *Catal. Today* **47**, 359 (1999).
24. Church, J. S., Cant, N. W., and Trimm, D. L., *Appl. Catal. A* **101**, 105 (1993).
25. Trimm, D. L., *in* "Handbook of Heterogeneous Catalysis" (G. Ertl, H. Knözinger, and J. Weitkamp, Eds.), Vol. 3, p. 1263. Wiley—VCH, Weinheim, 1997.
26. Groppi, G., Cristiani, C., Lietti, L., and Forzatti, P., *Stud. Surf. Sci. Catal.* **130**, 3801 (2000).
27. Farrauto, R. J., Hobson, M. C., Kennelly, T., and Waterman, E. M., *Appl. Catal. A* **81**, 227 (1992).
28. Talo, A., Lahtinen, J., and Hautojärvi, P., *Appl. Catal. B* **5**, 221 (1995).
29. Haack, L. P., deVries, J. E., Otto, K., and Chattha, M. S., *Appl. Catal. A* **82**, 199 (1992).
30. Bettman, M., Chase, R. E., Otto, K., and Weber, W. H., *J. Catal.* **117**, 447 (1989).
31. Ledford, J. S., Houalla, M., Proctor, A., Hercules, D. M., and Petrakis, L., *J. Phys. Chem.* **93**(18), 6770 (1989).
32. Trimm, D. L., *Appl. Catal.* **7**, 249 (1983).
33. Thevenin, P. O., Ersson, A., Kusar, H. J. M., Menon, P. G., and Järås, S. G., *Appl. Catal. A* **212**, 189 (2001).
34. Shyu, J. Z., Otto, K., Watkins, W. L. H., Graham, G. W., Belitz, R. K., and Gandhi, H. S., *J. Catal.* **114**, 23 (1988).
35. Otto, K., Haack, L. P., and de Vries, J. E., *Appl. Catal. B* **1**, 1 (1992).
36. Shelef, M., Haack, L. P., Soltis, R. E., de Vries, J. E., and Logothetis, E. M., *J. Catal.* **137**, 114 (1992).
37. Farrauto, R. J., Lampert, J. K., Hobson, M. C., and Waterman, E. M., *Appl. Catal. B* **6**, 263 (1995).
38. Lyubovsky, M., and Pfefferle, L., *Appl. Catal. A* **173**, 107 (1998).